HEPATOLOGY

HEPATOLOGY, VOL. 67, NO. 3, 2018

Hepatic Peroxisome Proliferator-Activated Receptor γ Coactivator 1β Drives Mitochondrial and Anabolic Signatures That Contribute to Hepatocellular Carcinoma Progression in Mice

Elena Piccinin,[1,2] Claudia Peres,[2] Elena Bellafante,[3] Simon Ducheix,[1,2] Claudio Pinto,[3] Gaetano Villani,[4] and Antonio Moschetta[1,5]

The peroxisome proliferator-activated receptor γ (PPARγ) coactivator-1β (PGC-1 β) is a master regulator of mitochondrial biogenesis and oxidative metabolism as well as of antioxidant defense. Specifically, in the liver, PGC-1β also promotes *de novo* lipogenesis, thus sustaining cellular anabolic processes. Given the relevant pathogenic role of mitochondrial and fatty acid metabolism in hepatocarcinoma (HCC), here we pointed to PGC-1β as a putative novel transcriptional player in the development and progression of HCC. For this purpose, we generated both hepatic-specific PGC-1β-overexpressing (LivPGC-1β) and PGC-1β knockout (LivPGC-1βKO) mice, and we challenged them with both chemical and genetic models of hepatic carcinogenesis. Our results demonstrate a pivotal role of PGC-1β in driving liver tumor development. Indeed, whereas mice overexpressing PGC-1β show greater tumor susceptibility, PGC-1β knockout mice are protected from carcinogenesis. High levels of PGC-1β are able to boost reactive oxygen species (ROS) scavenger expression, therefore limiting the detrimental ROS accumulation and, consequently, apoptosis. Moreover, it supports tumor anabolism, enhancing the expression of genes involved in fatty acid and triglyceride synthesis. Accordingly, the specific hepatic ablation of PGC-1β promotes the accumulation of ROS-driven macromolecule damage, finally limiting tumor growth. *Conclusion*: The present data elect hepatic PGC-1β as a transcriptional gatekeeper of mitochondrial function and redox status in HCC, orchestrating different metabolic programs that allow tumor progression. (HEPATOLOGY 2018;67:884-898)

SEE EDITORIAL ON PAGE 823

Hepatocellular carcinoma (HCC) is one of the six most common cancers and the third most frequent cause of cancer death.[1] Despite its morbidity, effective therapies for HCC are still limited, attributed to the poor understanding of the molecular mechanisms that are driving the cellular neoplastic transformation. Recently, it has been described that reprogrammed metabolism is one of the

Abbreviations: 8-Oxo-dG, 8-Oxo-2-deoxyguanosine; Abcb4, ATP binding cassette subfamily B member 4; ACC, acetyl-CoA carboxylase; AKT, protein kinase B; ALT, alanine aminotransferase; AST, aspartate aminotransferase; cDNA, complementary DNA; Col1a1, collagen type1 alpha1; DAB, 3,3'-diaminobezidine; DEN, diethylnitrosamine; DGAT1, diacylglycerol O-acyltransferase 1; FFAs, free fatty acids; β-HB, β-hydroxybutyrate; HCC, hepatocellular carcinoma; H&E, hematoxylin-eosin; HSCs, hepatic stellate cells; Il1β, interleukin-1β; LW/BW, liver/body weight ratio; NADPH, nicotinamide adenine dinucleotide phosphate; PBS, phosphate-buffered saline; PCNA, proliferating cell nuclear antigen; PGC-1β, peroxisome proliferator-activated receptor γ coactivator 1β; PI3K, phosphatidylinositol 3-kinase; PPARγ, peroxisome proliferator-activated receptor γ; Prdx3/5, peroxiredoxin 3 and 5; ROS, reactive oxygen species; SCD1, stearoyl-CoA desaturase 1; αSma, α-smooth muscle actin; Sod2, superoxide dismutase 2; TBP, TATA-binding protein; TGs, triglycerides; Tgf-β, transcription growth factor β; Tnf-α, tumor necrosis factor α; Txn2, thioredoxin 2; WT, wild type.

Received April 25, 2017; accepted August 28, 2017.

Additional Supporting Information may be found at onlinelibrary.wiley.com/doi/10.1002/hep.29484/suppinfo

A. Moschetta is funded by Italian Association for Cancer Research (AIRC; IG 18987), NR-NET FP7 Marie Curie ITN, and the Italian Ministry of Health (Young Researchers Grant GR-2010-2314703).

The Ethical Committee of the University of Bari approved this experimental setup, which also was certified by the Italian Ministry of Health in accordance with internationally accepted guidelines for animal care.

critical hallmarks of cancer pathogenesis.[2] Indeed, different molecular mechanisms concur to alter the metabolic processes required for the basal needs of rapidly dividing cancer cells.[3,4] Metabolic pathways are controlled at transcriptional level and they often depend on changes in the amounts or activities of transcription factors involved in their regulation.

The peroxisome proliferator-activated receptor γ (PPARγ) coactivator-1β (PGC-1β) belongs to the family of PGC-1 coactivators, considered the master regulators of mitochondrial biogenesis and oxidative metabolism as well as of antioxidant defense.[5] The coactivators, PGC-1α and PGC-1β, display a similar expression pattern, being highly expressed in tissues with an elevated mitochondrial energy metabolism, such as heart, skeletal muscle, and brown adipose tissue.[6-9] Nevertheless, the liver is possibly the organ that best illustrates the divergent role of PGC-1α and PGC-1β. Although both coactivators can modulate mitochondrial biogenesis, they can also regulate antagonistic physiological processes within the same tissue. Indeed, PGC-1α is mainly involved in gluconeogenesis,[10] whereas PGC-1β sustains *de novo* lipogenesis, thus supporting cell anabolism.[11,13] Given the relevance of mitochondrial metabolism and lipogenesis in HCC, our aim was to unravel the putative direct transcriptional role of PGC-1β in the development and progression of HCC.

To this end, we generated gain and loss of PGC-1β models and studied the tissue-specific role of this coactivator in liver metabolism and hepatocarcinogenesis. Our data depict an intriguing scenario where PGC-1β seems to act as an adaptive self-point regulator, able to provide balance between enhanced mitochondrial activity and antioxidant response, leading to a significant increase in tumor growth rate in the liver. Tumors may use adaptive mechanisms to keep their reactive oxygen species (ROS) burden within a range permitting growth and survival. In such contest, PGC-1β seems to act as a gatekeeper of redox status, allowing tumor progression.

Materials and Methods

GENERATION OF NOVEL MOUSE MODELS AND EXPERIMENTAL STUDIES

Hepatic-specific PGC-1β ablation (LivPGC-1βKO) was obtained by crossing AlbuminCre transgenic mice (The Jackson Laboratory, Bar Harbor, ME) with PGC-1β flox/flox (PGC-1$\beta^{fl/fl}$) mice. As a control group, we used PGC-1βfl/fl mice. LivPGC-1β transgenic mice were previously generated in our laboratory by Dr. E. Bellafante. These pure strain FVB/N mice display hepatic-specific PGC-1β overexpression.[11] We used wild-type (WT) FVB/N mice (referred as WT mice) as a control group. In the diethylnitrosamine (DEN)-induced HCC model, DEN (25 mg/kg) was injected intraperitoneally into 14-day-old male mice. Mice were successively killed after 10 months. Abcb4$^{-/-}$LivPGC-1β mice were generated by crossing LivPGC-1β transgenic mice with pure strain FVB/N Abcb4$^{-/-}$ mice (kindly provided by Prof. A.K. Groen, University of Amsterdam, Amsterdam, The Netherlands). Abcb4$^{-/-}$ mice were then used as a control group. Abcb4$^{-/-}$ mice represent a model of spontaneous hepatocarcinogenesis, because they generally

View this article online at wileyonlinelibrary.com.
DOI 10.1002/hep.29484

Potential conflict of interest: Nothing to report.

ARTICLE INFORMATION:

From the [1]Department of Interdisciplinary Medicine, "Aldo Moro" University of Bari, Bari, Italy; [2]INBB, National Institute for Biostuctures and Biosystems, Rome, Italy; [3]Fondazione Mario Negri Sud, Santa Maria Imbaro, Chieti, Italy; [4]Department of Basic Medical Sciences, Neurosciences and Sense Organs, "Aldo Moro" University of Bari, Bari, Italy; and [5]National Cancer Center, IRCCS "Giovanni Paolo II", 70124 Bari, Italy.

ADDRESS CORRESPONDENCE AND REPRINT REQUESTS TO:

Antonio Moschetta, M.D. Ph.D.
Section of Internal Medicine "Cesare Frugoni",
Department of Interdisciplinary
Medicine, University of Bari "Aldo Moro"
Piazza Giulio Cesare 11
70124 Bari, Italy
E-mail: antonio.moschetta@uniba.it
Tel: + 39 0805593262

develop liver tumor after 14 months of life. Abcb4$^{-/-}$LivPGC-1β and control mice were killed after 14-15 months from birth. All mice were killed, and their livers were removed. Macroscopical inspection and liver gross morphology evaluation were performed. Externally visible tumors (>1 mm) were counted and measured. Samples of liver tumors were either crushed in liquid nitrogen or fixed in 10% formalin solution at room temperature. All the experiments presented in this work were carried out in male mice. All mice were housed under pathogen-free conditions in a temperature-controlled room (23°C) on a 12-hour light/dark cycle and consumed water *ad libitum*. The Ethical Committee of the University of Bari (Bari, Italy) approved this experimental setup, also certified by the Italian Ministry of Health in accordance with internationally accepted guidelines for animal care.

RNA EXTRACTION AND REAL-TIME qPCR

Tissues were crushed under liquid nitrogen to allow homogenization through a Qiagen TissueLyser (Qiagen, Hilden, Germany). Total RNA was isolated by QIAzol reagent (Qiagen), following the manufacturer's instruction. To avoid possible DNA contaminations, RNA was treated with DNAase (Thermo Fisher Scientific, Waltham, MA). RNA purity was checked by a spectrophotometer and RNA integrity by examination on agarose gel electrophoresis. Complementary DNA (cDNA) was synthesized by retro-transcribing 4 μg of total RNA in a total volume of 100 μL using the High Capacity DNA Kit (Thermo Fisher Scientific), following the manufacturer's instruction. The sequences of validated primers used to detect mRNA expression levels for the genes investigated in this study are available upon request. PCR assays were performed in 96-well optical reaction plates using the QuantStudio5 machine (Thermo Fisher Scientific). PCR assays were conducted in triplicate wells for each sample. The following reaction mixture per well was used: 10 μL of Power Syber Green (Thermo Fisher Scientific); 2.4 μL of primers at the final concentration of 150 nM; 4.6 μL of RNase free water; and 3 μL of cDNA. For all experiments, the following PCR conditions were used: denaturation at 95°C for 10 minutes, followed by 40 cycles at 95°C for 15 seconds and at 60°C for 60 seconds. Quantitative normalization of cDNA in each sample was performed using TBP (TATA-binding protein) mRNA as an internal control. Relative quantification was done using the delta-delta threshold cycle method.

SERUM ANALYSIS

Blood samples were collected in lithium-heparin collection tubes at the time of the sacrifice. Samples were then centrifuged in order to obtain serum. Serum levels of alanine aminotransferase (ALT) and aspartate aminotransferase (AST) were measured with a colorimetric kit (BioQuant, Heidelberg, Germany), according to manufacturer's instructions. The assessment of serum free fatty acids (FFAs) and β-hydroxybutyrate (β-HB) was performed using a colorimetric kit (Abcam, Cambridge, UK).

LIVER AND PLASMA LIPID CONTENT

Liver triglycerides (TGs) and cholesterol were extracted using the Folch method. Briefly, liver tissue (around 100 mg) was homogenized in 5 mL of chloroform/methanol 2:1 (v/v) and washed twice with 1 mL of 0.36 M $CaCl_2$/methanol. TGs and cholesterol were measured with a colorimetric kit (Sentinel Diagnostic, Milan, Italy), according to the manufacturer's instructions.

HISTOLOGY AND IMMUNOHISTOCHEMISTRY

Tissue specimens were fixed in 10% formalin for 12-24 hours, dehydrated, and paraffin embedded. Sections (4 µm thick) were stained with hematoxylin-eosin (H&E), following standard protocols. Liver fibrosis was analyzed with Sirius Red by using Direct Red 80 and Fast Green FCF (Sigma-Aldrich, St Louis, MO). Briefly, sections were subjected to antigen retrieval by boiling the slides in sodium citrate (pH 6; Sigma-Aldrich) for 15min. Sections were permeabilized in phosphate-buffered saline (PBS) with 0.25% Triton X-100 for 5 min and were sequentially incubated for 10min at room temperature in protein blocking solution (Dako, Glostrup, Denmark) followed by an overnight to 48 hours incubation at 4°C with the primary antibodies (anti-PCNA [proliferating cell nuclear antigen], Santa Cruz Biotechnology, Dallas, TX; anti-8-hydroxyguanosine, LifeSpan Bioscience Inc, Seattle, WA). Sections were washed in PBS for 15 minutes and incubated for 25 minutes at room temperature with DAKO real EnVision detection

system Peroxidase/DAB + (Dako), according to the manufacturer's instruction. After washing in PBS, the peroxidase reaction was initiated by incubation with 3,3'-diaminobezidine (DAB; Dako). Coverslips were mounted with Permount and evaluated under a light microscope.

Specimens from livers were embedded in optimal cutting temperature compound (Tissue-Tek Sakura, Torrance, CA) and stored at −80°C. Serial 4.5-μm cryosections of liver were stained with Oil Red O (Sigma-Aldrich) and hematoxylin to counterstain nuclei.

Image processing was performed using ImageJ (NIH, Bethesda, MD) software. For each sample, 10 representative images were taken with a 20 × objective. The percentage of stained area/total area was measured. Values from all consecutive images for each sample were averaged. For negative controls, 1% nonimmune serum in PBS replaced the primary antibodies.

WESTERN BLOTTING ANALYSIS

Equal amounts of total tissue lysates (50 μg) were separated on a 7% or 10% sodium dodecyl sulfate/polyacrylamide gel and transferred onto nitrocellulose membrane. Membranes were blocked with 5% bovine serum albumin in Tris-buffered saline/0.01% Tween 20 and probed with specific antibodies against PGC-1β (home-made antibody), diacylglycerol O-acyltransferase 1 (DGAT1; Abcam), acetyl-CoA carboxylase (ACC), stearoyl-CoA desaturase 1 (SCD1), total AKT (protein kinase B), phospho-AKT (Ser473), total p70S6K, and phospho-p70S6K (Cell Signaling Technlogy, Danvers, MA). Nuclear encoded β-actin (Abcam) or glyceraldehyde 3-phosphate dehydrogenase (Santa Cruz Biotechnology) were used as loading control. Membranes were finally incubated with horseradish peroxidase–conjugated secondary antibodies and developed with a chemiluminescent reagent (Bio-Rad Laboratories, Hercules, CA).

STATISTICAL ANALYSIS

All results are expressed as mean ± SEM. Data distribution and gene expression statistical analysis were performed with GraphPad Prism software (v5.0; GraphPad Software Inc., La Jolla, CA). Comparisons of two groups were performed using a Student t test followed by the Mann-Whitney U test. A value of $P < 0.05$ was considered as statistically significant.

Results

HEPATIC PGC-1β OVEREXPRESSION PROMOTES CHEMICALLY INDUCED HEPATOCARCINOGENESIS

To study the role of PGC-1β in the development and progression of HCC, we used a chemically induced model of HCC in mice overexpressing PGC-1β in the liver (Supporting Fig. S1A). We injected LivPGC-1β mice and WT littermates with a single intaperitoneal injection of DEN (25 mg/kg). This carcinogen triggers DNA damage, cell death responses, and compensatory proliferation in the liver.[12] At 6 months of age, 60% of LivPGC-1β mice injected with DEN showed small tumor formation; in contrast, none of the WT mice developed tumors (Supporting Fig. S1B). At 10 months of age, untreated mice revealed no spontaneous tumors, whereas all DEN-treated mice developed typical HCC. Gross morphology and histological analysis of the liver revealed deteriorated tumor dysplasia in LivPGC-1β mice (Fig. 1A,F). Strikingly, the number and maximal size of detectable tumors was 3-fold and 2-fold higher in LivPGC-1β mice compared to WT, respectively (Fig. 1B). In agreement, LivPGC-1β mice exhibited an increase in liver/body weight ratio (LW/BW) and in serum ALT and AST levels, compared to controls (Fig. 1C-E). Correspondingly, compared to WT mice, LivPGC-1β mice displayed elevated expression of proliferation (PCNA) and tumor (cyclin E) markers (Fig. 1F-H), whereas no difference in the involvement of phosphatidylinositol 3-kinase (PI3K)/AKT pathway was detected (Supporting Fig. S1C). Recently, it has been demonstrated that collagen is actively involved in promoting tumor progression, by destabilizing cell polarity and cell-cell adhesion and increasing growth factor signaling.[14] Hepatic stellate cells (HSCs) are predominantly in charge of collagen fiber deposition in the extracellular matrix and are usually activated in highly fibrotic liver.[15,16] Given that HCC usually develops from cirrhosis, we evaluated the HSC activation and collagen deposition in the liver tumor specimens. Liver expression of Tgf-β (transcription growth factor β) and αSma (α-smooth muscle actin), two markers associated with HSC activation, were higher in LivPGC-1β mice compared to the control group (Fig. 1I-L). Accordingly, transgenic mice displayed increased collagene synthesis and deposition, as

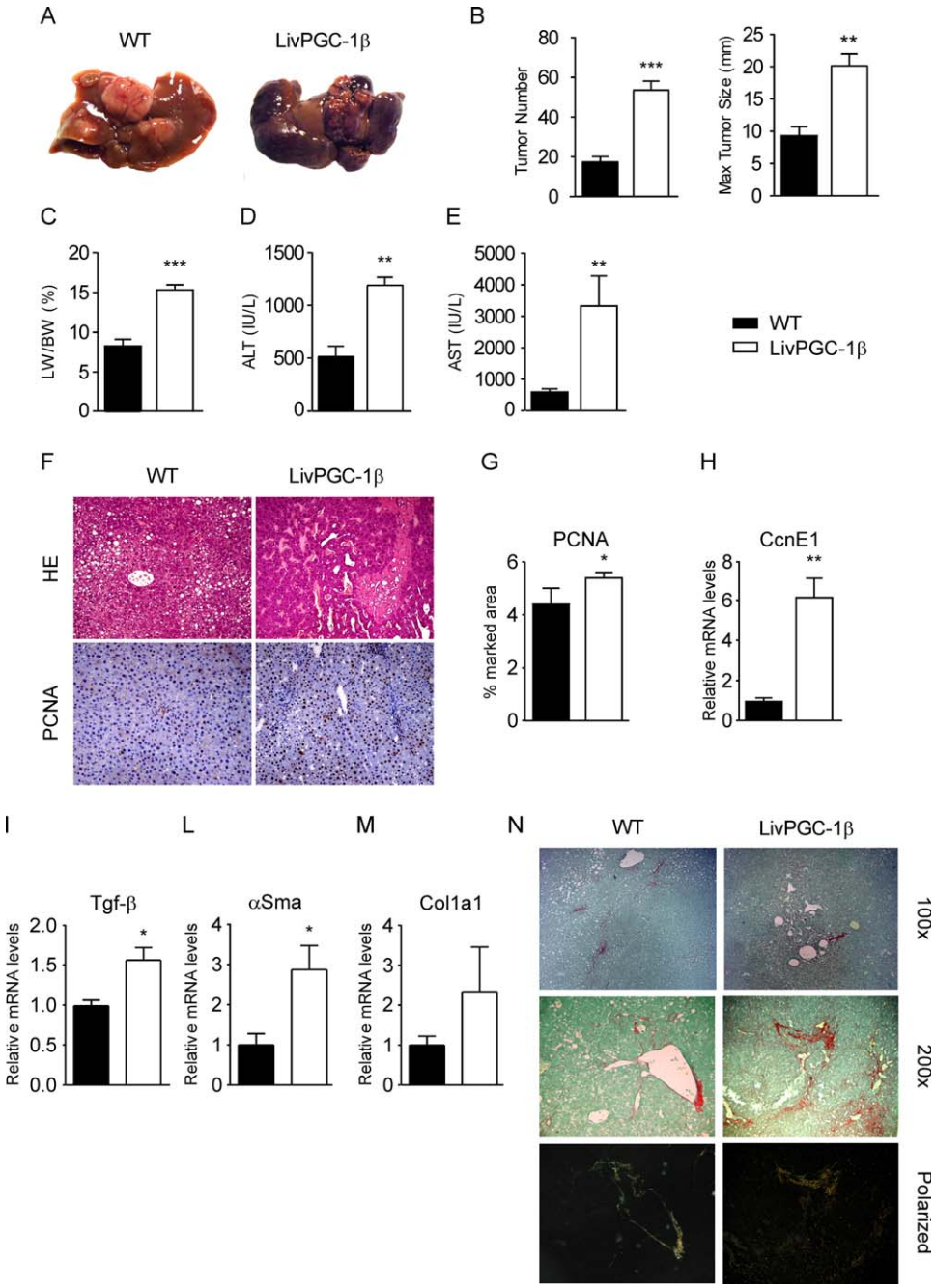

FIG. 1. Hepatic PGC-1β overexpression promotes and sustains chemical hepatocarcinogenesis. Fourteen-day-old mice overexpressing PGC-1β specifically in the liver (LivPGC-1β) and WT littermates were injected with DEN and killed 10 months later. (A) Gross morphology of livers in mice of indicated genotype. (B) Tumor numbers and maximal tumor sizes of WT and LivPGC-1β mice. (C) LW/BW and serum (D) ALT and (E) AST of WT and LivPGC-1β mice developed liver tumors. (F) Staining of liver sections from WT and LivPGC-1β mice with H&E and PCNA (magnification, 200×). (G) Bar graphs indicate percentage of PCNA positive area per field. (H) Relative CyclinE expression evaluated by real-time qPCR. LivPGC-1β tumors displayed elevated HSC activation, as indicated by (I) Tgf-β and (L) αSma expression. Hence collagen expression (M) and deposition, as indicated by Sirius Red staining (N) are higher in LivPGC-1β mice. Relative gene expression was evaluated in liver specimens from WT mice and LivPGC-1β mice by real-time qPCR, using TBP as a housekeeping gene. Comparison of WT and transgenic mice (n = 10) was performed using a Student *t* test followed by Mann-Witney U test. Results are expressed as mean ± SEM (*$P < 0.05$; **$P < 0.01$; ***$P < 0.001$). Abbreviation: CcnE1, cyclin E1.

indicated by Col1a1 (collagen type1 alpha1) expression levels and Sirius Red staining, respectively (Fig. 1M,N). Sirius Red staining visualization under polarized light allowed us to discriminate between larger collagen fibers (bright red or orange) and thinner ones, including reticular fibers (green). Interestingly, LivPGC-1β liver tumors were characterized by large collagen fibers compared to WT (Fig. 1N), thus indicating a worse tumor phenotype in transgenic mice. Taken together, these data clearly indicate that hepatic overexpression of PGC-1β plays a prominent role in development and progression of hepatic tumorigenesis.

PGC-1β PROMOTES LIVER TUMORIGENESIS BY ENHANCING ROS DETOXIFICATION PROGRAM AND SUSTAINING FATTY ACIDS METABOLISM IN HCC

ROS are mutagenic and may stimulate tumorigenesis through oxidation of DNA and subsequent accumulation of mutations in key genes involved in cell cycle and proliferation as well as in carcinogenesis.[17,18] However, it has been recently demonstrated that the oncogene-induced activation of a ROS-detoxification program, leading to a low level of ROS, enhances tumorigenesis.[3,19] Expression of ROS scavengers is tightly associated with expression of PGC-1β[11,20] (Supporting Fig. S2A). Indeed, real-time qPCR analysis revealed that the PGC-1β ability to foster ROS scavenger expression was still retained in tumors from LivPGC-1β mice, with the levels of Sod2 (superoxide dismutase 2), Prdx3 (peroxiredoxin 3), Prdx5 (peroxiredoxin 5), and Txn2 (thioredoxin 2) being enhanced in transgenic mice compared to WT littermates (Fig. 2A). Moreover, the immunohistochemical analysis of 8-Oxo-2-deoxyguanosine (8-Oxo-dG), a marker of ROS-dependent DNA damage, displayed a low level of ROS injury in LivPGC-1β mice tumors (Fig. 2B,C). Overall, these data confirm that, in the present model, tightly controlled ROS levels are associated with sustained tumor growth, thus supporting the role of PGC-1β as a master regulator of the antioxidant system in the liver.

Given that increased lipid metabolism is now considered a remarkable feature of cancer metabolism and given that one of the central roles of PGC-1β in liver is related to its ability to support lipogenesis and TG secretion[11,13,21] (Supporting Fig. S2B), we wondered whether PGC-1β overexpression would be able to confer metabolic advantage to tumor growth, possibly increasing fatty acid metabolism. We observed a significant induction of Acc, a gene involved in *de novo* lipogenesis, in LivPGC-1β mice compared to WT controls (Fig. 2D,G). Moreover, expression of the major enzyme involved in TG synthesis, Dgat1, was strongly increased in LivPGC-1β mice compared to control ones (Fig. 2E,G). Finally, overexpression of PGC-1β in the liver was also able to induce the expression of Scd1, an enzyme that produces monounsaturated fatty acids (Fig. 2F,G). Lipidomic analysis studies have revealed that a shift toward polyunsaturated fatty acids chain composition is observed in an aggressive and invasive form of tumor.[22] Thus, the increased Scd1 expression could be related to higher malignancies of LivPGC-1β tumor.[23] No significant differences were detected in other genes involved in fatty acid metabolism both in tumor and in saline-treated mice (Supporting Figs. S1D and S2B). Interestingly, mice overexpressing PGC-1β displayed a high TGs turnover. Indeed, LivPGC-1β mice presented a marked reduction of hepatic TG (Figure 2H) and a concomitant significant increase in serum TG (Fig. 2M). Hepatic cholesterol content did not show any difference (Fig. 2I), whereas a marked elevation in circulating cholesterol levels was observed in LivPGC-1β compared to WT (Fig. 2N). Hepatic lipid content was also confirmed by Red Oil staining, revealing only small lipid droplets retention within hepatocytes of LivPGC-1β mice, in contrast with a massive accumulation of macrovescicular lipid droplets in WT mice (Fig. 2L).

Consistent with previous studies in which hepatic PGC-1β overexpression was able to counteract hepatocyte cell death attributed to lipid accumulation under high-fat diet feeding by promoting TG clearance through mitochondrial β-oxidation,[11] we found that the ability of PGC-1β to drive fatty acids oxidation was still retained in tumors. Indeed, LivPGC-1β mice displayed a slight increase in serum FFAs together with a marked increase of serum β-HB (Supporting Fig. S1E). However, no significant difference in PPARα expression levels was detected in LivPGC-1β mice (Supporting Fig. S1D).

HEPATIC PGC-1β OVEREXPRESSION SUPPORT TUMOR GROWTH IN A GENETIC MODEL OF HEPATOCARCINOGENESIS

The mechanism of the hepatocarcinogenic action of DEN is based on a primary generation of ROS upon bioactivation of the detoxifying cytochrome P450, causing hepatocyte death.[24] HCC development in this model usually follows a slow multistep sequence, where cycles of necrosis and regeneration ultimately promote neoplastic transformation. The progression from early dysplastic lesions to fully malignant tumors is associated with an increased occurrence of genomic alteration. Although PGC-1β seems to promote tumor phenotype not in an oncogene-dependent manner, but

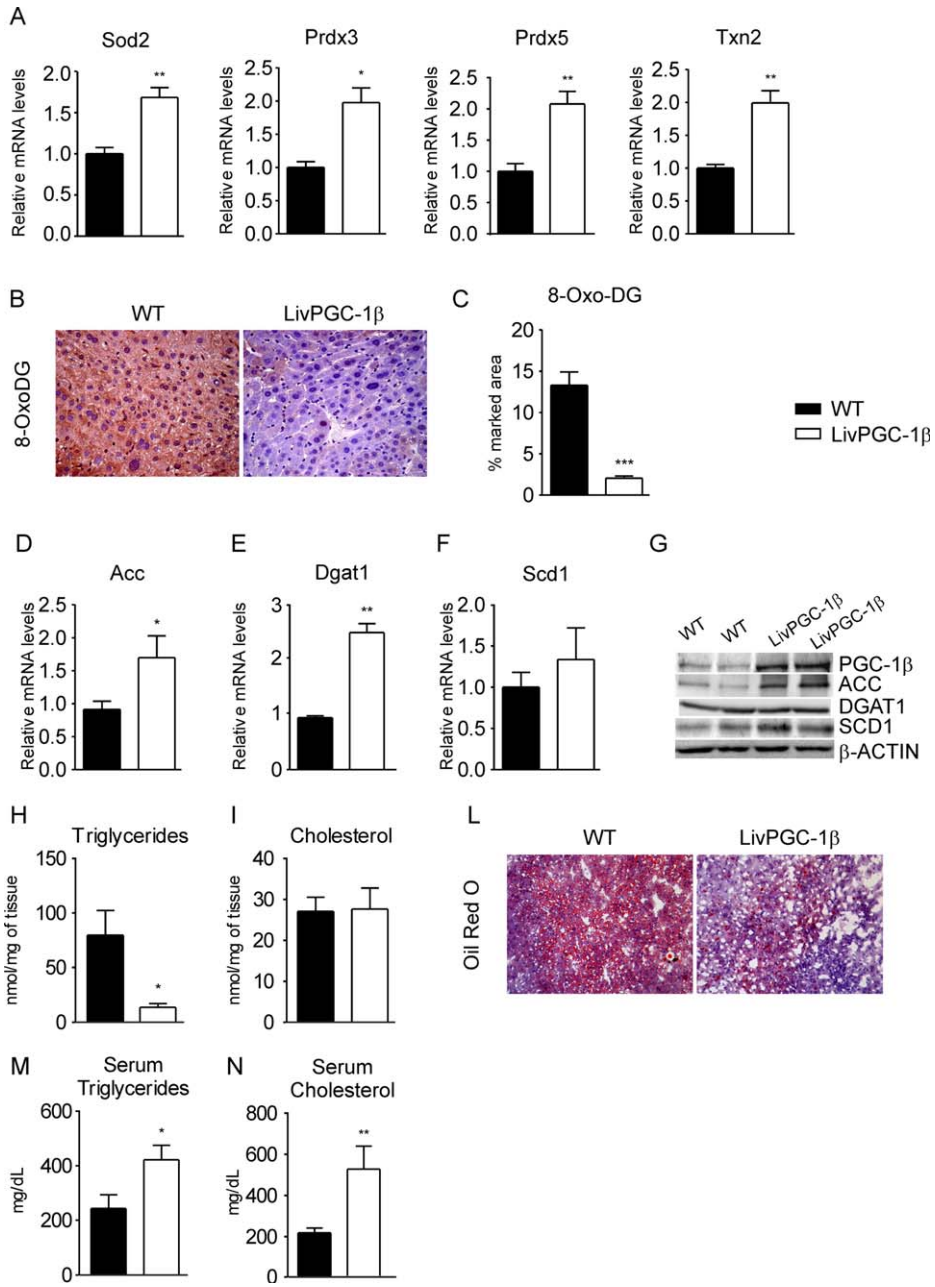

FIG. 2. PGC-1β promotes liver tumorigenesis, enhancing ROS detoxification program and fostering fatty acid metabolism. (A) Expression of ROS scavengers Sod2, Prdx3, Prdx5, and Txn2 was measured in liver tumor specimens from WT and LivPGC-1β mice by real-time qPCR, using Tbp as a housekeeping gene. (B) 8-oxo-dG levels were evaluated by immunohistochemistry (magnification, 400×). Bar graphs indicate percentage of (C) 8-Oxo-dG positive area per field. Relative mRNA expression of genes involved in (D,E,F) *de novo* lipogenesis and TGs synthesis evaluated in liver tumor specimens from WT mice and LivPGC-1β mice by real-time qPCR using Tbp as a housekeeping gene, and then confirmed by western blotting analysis (G) of PGC-1β, ACC, DGAT1, and SCD1 on liver samples from WT mice and LivPGC-1β mice. Hepatic TGs (H) and cholesterol (I) were extracted from frozen liver tumor specimens and measured with the colorimetric method. (L) Frozen cryostat section (10 μm thick) from tumor specimens of WT and LivPGC-1β mice were stained with Oil Red O staining that marks neutral lipid (magnification, 200×). Serum TGs (M) and cholesterol (N) levels were measured in WT and LivPGC-1β mice. Comparison of WT and transgenic mice (n = 10) was performed using a Student *t* test followed by Mann-Witney U test. Results are expressed as mean ± SEM ($^{*}P < 0.05$; $^{**}P < 0.01$; $^{***}P < 0.001$).

rather by enhancing the reprogramming of energy metabolism, the independence from genetic alterations driving HCC development is still to be addressed. Therefore, we decided to use a genetic mouse model, in which the expression of ATP binding cassette subfamily B member 4 (Abcb4) gene is impaired. Abcb4 is coding the multidrug resistance 2 protein, a phospholipid flippase which promotes biliary secretion of phosphatidylcholine, and its genetic alterations have been associated with several diseases, such as cirrhosis and familial intrahepatic cholestasis.[25] In Abcb4$^{-/-}$ mice, liver inflammation and toxicity induced by deregulation of pathways related to oxidative stress and lipid metabolism lead to hepatocyte dysplasia, evolving in HCC at 14-16 months of age.[26,27] To study whether PGC-1β overexpression is able to sustain tumor growth and development also in an inflammation-associated model of HCC, we crossed LivPGC-1β mice with Abcb4$^{-/-}$ mice in order to obtain mice that specifically overexpress PGC-1β in liver in an Abcb4 null background (Abcb4$^{-/-}$LivPGC-1β). Tumor lesions at 6 months of age were detected

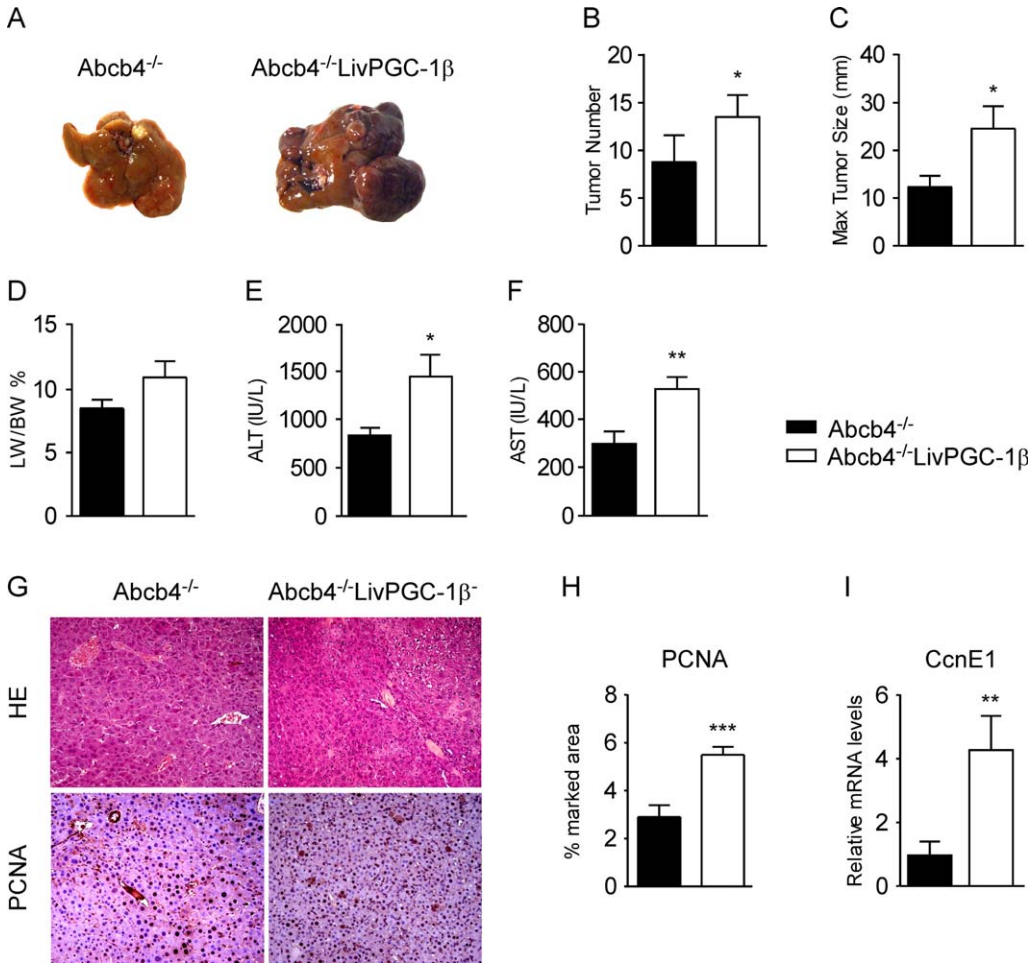

FIG. 3. Hepatic PGC-1β overexpression promotes and sustains hepatocarcinogenesis in the genetic Abcb4$^{-/-}$ mouse model. Abcb4$^{-/-}$ mice and mice with hepatic-specific PGC-1β overexpression in Abcb4$^{-/-}$ background (Abcb4$^{-/-}$LivPGC-1β) were sacrificed 14 months after birth. (A) Gross morphology of livers in mice of indicated genotype. (B) Tumor numbers and (C) maximal tumor sizes of Abcb4$^{-/-}$ and Abcb4$^{-/-}$LivPGC-1β mice. (D) LW/BW and serum (E) ALT and (F) AST of Abcb4$^{-/-}$ and Abcb4$^{-/-}$LivPGC-1β mice with developed liver tumors. (G) Staining of liver sections from Abcb4$^{-/-}$ and Abcb4$^{-/-}$LivPGC-1β mice with H&E and PCNA (magnification, 200×). (H) Bar graphs indicate percentage of PCNA-positive area per field. (I) Relative CyclinE expression evaluated by real-time qPCR in liver specimens of Abcb4$^{-/-}$ and Abcb4$^{-/-}$LivPGC-1β mice, using TBP as a housekeeping gene. Comparison of Abcb4$^{-/-}$ and Abcb4$^{-/-}$LivPGC-1β mice (n = 10) was performed using a Student t test followed by Mann-Witney U test. Results are expressed as mean ± SEM (*$P < 0.05$; **$P < 0.01$; ***$P < 0.001$). Abbreviation: CcnE1, cyclin E1.

only in Abcb4$^{-/-}$LivPGC-1β mice (10%; Supporting Fig. S3A). Accordingly, liver gross morphology (Fig. 3A) and histological analysis (Fig. 3D) in 14-month-old mice revealed that hepatic overexpression of PGC-1β deteriorated tumor phenotype. Indeed, the number of tumors detected in Abcb4$^{-/-}$LivPGC-1β mice and their size were dramatically increased compared to Abcb4$^{-/-}$ controls (Fig. 3B,C). As shown in the DEN model, Abcb4$^{-/-}$LivPGC-1β mice displayed higher LW/BW, together with a significant elevation of ALT and AST serum levels, compared to control mice (Fig. 3D-F). Expression of the tumor markers, cyclin E and PCNA, was markedly up-regulated in Abcb4$^{-/-}$LivPGC-1β mice (Fig. 3G-I).

PGC-1β ENHANCES TUMOR PROLIFERATION THROUGH SUSTAINING METABOLIC REPROGRAMMING IN Abcb4 NULL MICE

Because we have previously demonstrated that PGC-1β overexpression is able to support tumor growth and proliferation, promoting both antioxidant response and fatty acid biosynthesis, and given that Abcb4 null mice are characterized by impaired ROS production and *de novo* lipogenesis,[27,28] we wondered whether the high rate of tumor growth displayed in Abcb4$^{-/-}$LivPGC-1β mice could be related to the ability of PGC-1β to revert the Abcb4 *null* tumor phenotype, by enhancing metabolic reprogramming in malignant cells.

First, we evaluated the antioxidant response, revealing that PGC-1β boosts expression of ROS scavengers (Fig. 4A), hence contrasting the cellular accumulation of reactive molecules. The immunohistochemical assessment of ROS by-products clearly displayed a marked decrease of 8-Oxo-dG in Abcb4$^{-/-}$LivPGC-1β mice compared to controls (Fig. 4B,C). These data confirm, once again, the prominent role of PGC-1β in sustaining antioxidant response and therefore cell longevity.

Next, we analyzed the PGC-1β contribution in fostering fatty acid synthesis for the anabolic needs of tumour cell growth. Expression of the lipogenic enzymes, Acc and Dgat1, was significantly up-regulated in liver tumors of Abcb4$^{-/-}$LivPGC-1β in comparison to controls (Fig. 4E,D and Supporting Fig. S3B). Moreover, a trend to increase Scd1 expression was also observed upon PGC-1β overexpression (Fig. 4F and Supporting Fig. S3B). Then, a significantly increased expression of the genes involved in the fatty acids synthesis, Fasn (fatty acids synthase) and TGs production, Lipin1a and Gpam (glycerol-3-phosphate acyltransferase 1, mitochondrial), was detected in mice overexpressing PGC-1β (Supporting Fig. S3C). No significant change in expression levels of ME, Lipin1b, and PPARα was observed (Supporting Fig. S3C). Nevertheless, we noticed a decreased expression of PGC-1α (Supporting Fig. S3C), together with a marked down-regulation of lipid content, as indicated by few macrovescicular lipid droplets found within the hepatocytes of Abcb4$^{-/-}$LivPGC-1β mice compared to a massive retention of neutral lipids in Abcb4$^{-/-}$ liver detected by Red Oil staining (Fig. 4I). Hepatic TG content showed a trend toward reduction in Abcb4$^{-/-}$LivPGC-1β mice, along with a slight increase of serum TG levels (Fig. 4G,L), whereas serum and hepatic cholesterol levels were not affected (Fig. 4H,M), confirming a prevalent role of PGC-1β coactivator in the hepatic TG turnover. The serum level of β-HB was mildly increased in PGC-1β-overexpressing mice, although no differences were detected in circulating FFA (Supporting Fig. S3D). Overall, these data fully confirm the effects of PGC-1β overexpression in a genetic model of liver carcinogenesis.

ABSENCE OF HEPATIC PGC-1β PROTECTS MICE FROM HCC DEVELOPMENT

In order to corroborate our data with the loss-of-function proof, we generated mice lacking hepatic expression of PGC1-β (LivPGC-1βKO; Fig. 5A,B and Supporting Fig. S4A). These mice, under basal conditions, displayed lower expression of genes involved in ROS scavenging, whereas no significant difference was found in the expression of lipogenic enzymes (Fig. 5C-E and Supporting Fig. S4B). Thus, in order to validate the cancer-driving role of PGC-1β, we challenged LivPGC-1βKO mice with DEN. Gross morphology analysis of the liver revealed fewer and smaller tumors in LivPGC-1βKO mice compared to the PGC-1$\beta^{fl/fl}$ control group (Fig. 6A-C). Moreover, LivPGC-1βKO mice displayed a more preserved hepatic parenchyma compared to PGC-1$\beta^{fl/fl}$ control mice, characterized by less necrotic areas and inflammatory infiltrates (Fig. 6G). Although there were no substantial differences in the LW/BW (Fig. 6D), ALT and AST markers of liver injury were both

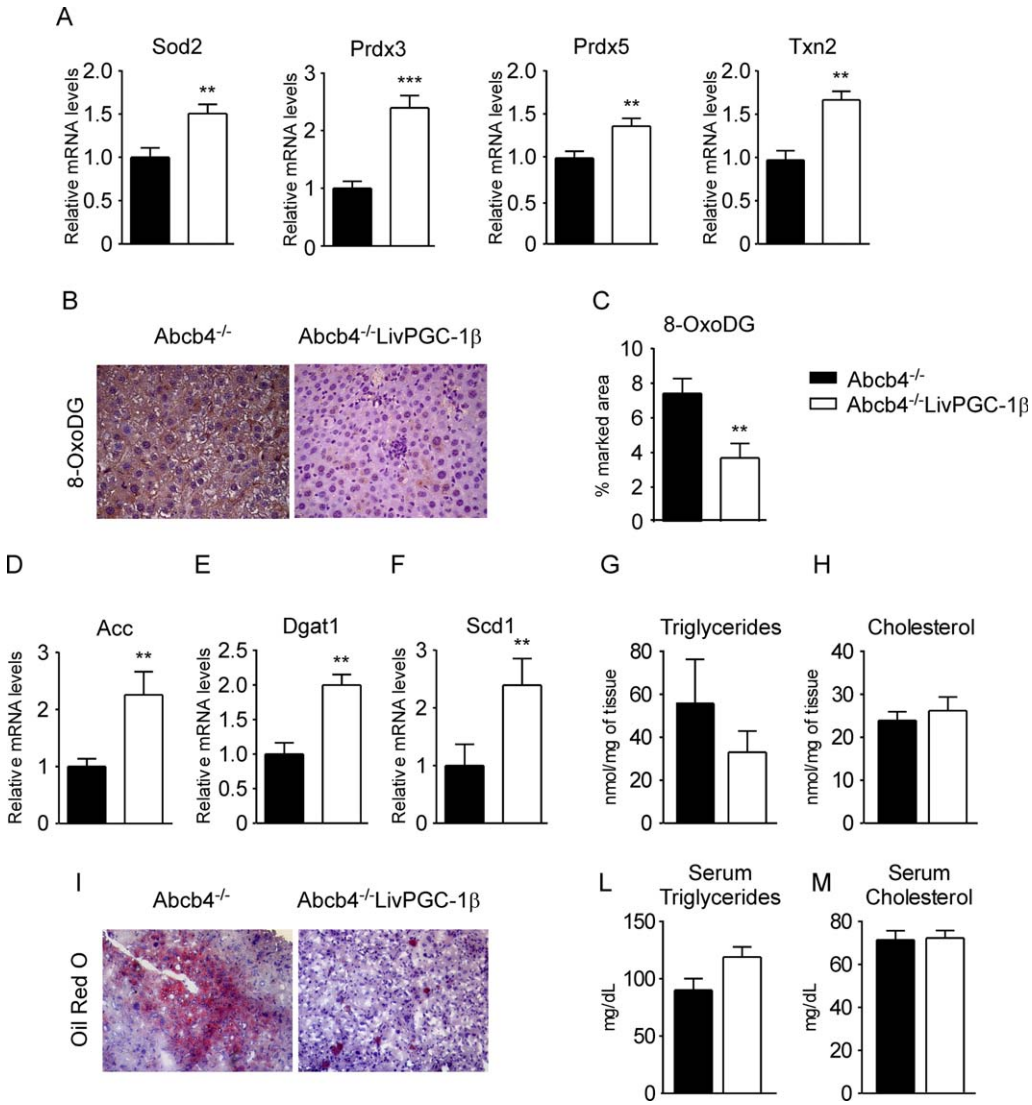

FIG. 4. PGC-1β supports ROS detoxification program in genetic model of hepatocarcinogenesis. (A) Expression of ROS scavengers Sod2, Prdx3, Prdx5, and Txn2 was measured in liver tumor specimens from Abcb4$^{-/-}$ and Abcb4$^{-/-}$LivPGC-1β mice by real-time qPCR, using TBP as a housekeeping gene. (B) 8-oxo-dG levels were evaluated by immunohistochemistry (magnification, 400×). Bar graphs indicate percentage of (C) 8-Oxo-dG-positive area per field. Relative mRNA expression of genes involved in *de novo* lipogenesis and TG synthesis (D,E,F) evaluated in liver tumor specimens from Abcb4$^{-/-}$ and Abcb4$^{-/-}$LivPGC-1β mice by real-time qPCR using TBP as a housekeeping gene. Hepatic TGs (G) and cholesterol (H) were extracted from frozen liver tumor specimens and measured with the colorimetric method. (I) Frozen cryostat section (10 μm thick) from tumor specimens of Abcb4$^{-/-}$ and Abcb4$^{-/-}$LivPGC-1β mice were stained with Oil Red O staining that marks neutral lipid (magnification, 200×). Serum TGs (L) and cholesterol (M) levels were measured in Abcb4$^{-/-}$ and Abcb4$^{-/-}$LivPGC-1β mice. Comparison of Abcb4$^{-/-}$ and Abcb4$^{-/-}$LivPGC-1β mice (n = 10) was performed using a Student *t* test followed by Mann-Witney U test. Results are expressed as mean ± SEM (*$P < 0.05$; **$P < 0.01$; ***$P < 0.001$).

dramatically decreased in serum of mice lacking hepatic PGC-1β expression (Fig. 6E,F). No changes were observed in cyclin E and PCNA expression (Fig. 6G-I) and in the PI3K/AKT pathway (Supporting Fig. S4C).

We next examined the extent of liver fibrosis, and we found less Sirius Red–positive areas in LivPGC-1βKO, compared to control mice, that appeared green under polarized light, thus ascribing the staining to the finest reticular collagene fibers (Fig. 7A). Additionally,

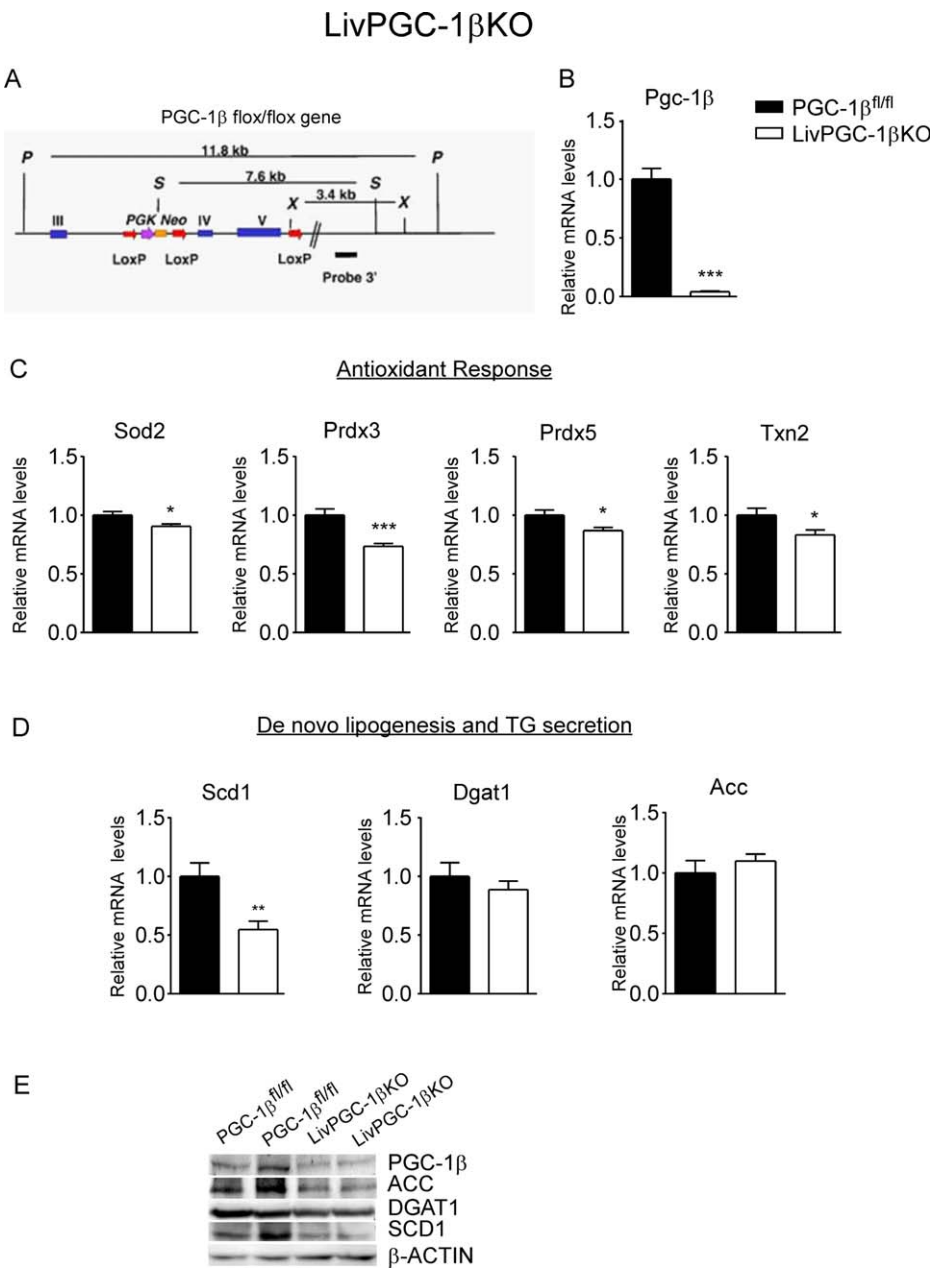

FIG. 5. Hepatic-specific PGC-1β ablation impairs lipid metabolism and antioxidant response. (A) Schematic representation of PGC-1β flox/flox gene.[38] (B) PGC-1β mRNA expression is almost absent in LivPGC-1βKO mice, and this affects the expression of genes involved in (C) antioxidant response as well as in (D) *de novo* lipogenesis and TG secretion. Relative gene expression was evaluated in liver specimens from PGC-1$\beta^{fl/fl}$ mice and LivPGC-1βKO mice by real-time qPCR, using TBP as a housekeeping gene. Western blotting analysis (E) of PGC-1β, ACC, DGAT1, and SCD1 on liver samples from PGC-1$\beta^{fl/fl}$ mice and LivPGC-1βKO mice. Comparison of PGC-1$\beta^{fl/fl}$ mice and LivPGC-1βKO mice (n = 12) was performed using a Student *t* test followed by Mann-Witney U test. Results are expressed as mean ± SEM (*$P < 0.05$; **$P < 0.01$; ***$P < 0.001$). Abbreviation: kb, kilobases.

hepatic gene expression analysis showed a trend toward a reduction of Col1a1 and αSma levels in LivPGC-1βKO mice (Fig. 7B,C). Given the central role of inflammatory response in mediating collagen deposition, and therefore HCC development,[16] we assessed the hepatic cytokine content upon PGC-1β ablation in the liver, and we detected a mild reduction of interleukin-1β (Il1β), together with a significant decrease of tumor necrosis factor α (Tnf-α) and Tgf-β transcripts in LivPGC-1βKO mice compared to controls (Fig. 7D-F).

Moreover, livers of LivPGC-1βKO mice were more susceptible to oxidative stress, as demonstrated by increased 8-Oxo-dG staining (Fig. 7H-I), compared to control mice. Interestingly, despite the high levels of 8-Oxo-dG observed in the cytosol of both groups, mostly attributed to the contribution of mitochondrial DNA, the modified base was markedly accumulated in

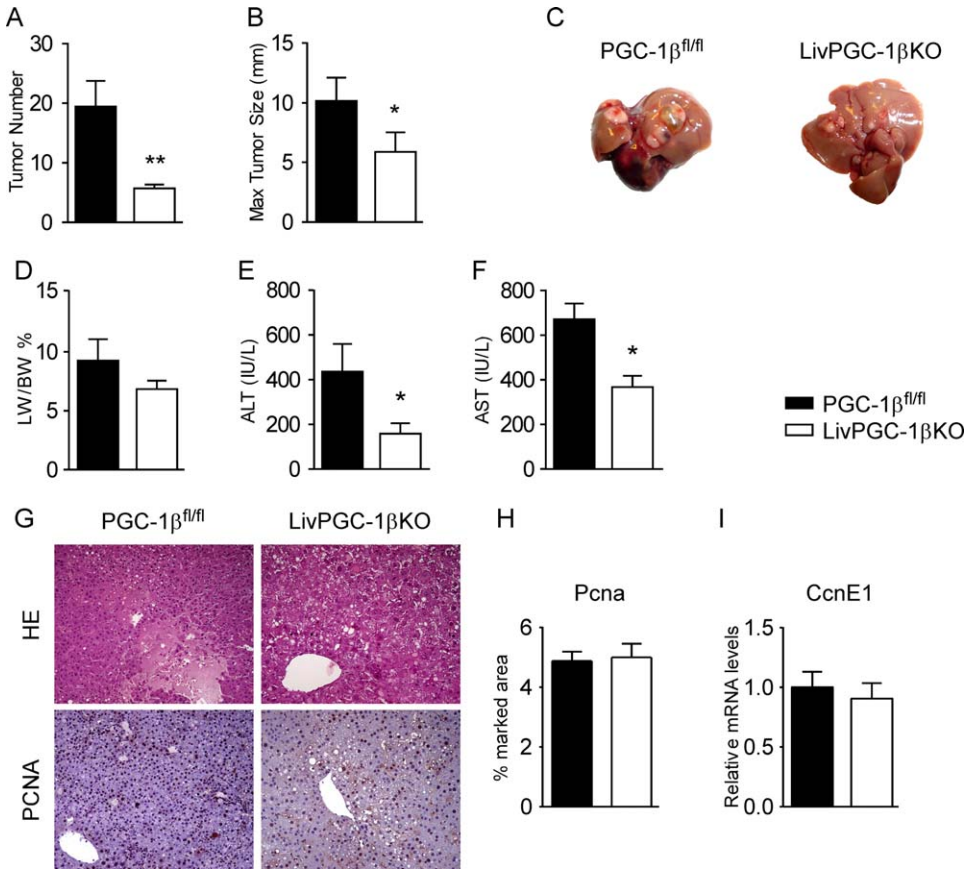

FIG. 6. Hepatic-specific PGC-1β ablation protects mice from HCC development. Mice lacking PGC-1β expression specifically in the liver (LivPGC-1βKO) and control littermates (PGC-1$\beta^{fl/fl}$) were injected with DEN and killed 10 months later. (A) Tumor numbers and (B) maximal tumor sizes of PGC-1$\beta^{fl/fl}$ and LivPGC-1βKO mice. (C) Gross morphology of livers in mice of indicated genotype. (D) LW/BW and serum (E) ALT and (F) AST of PGC-1$\beta^{fl/fl}$ and LivPGC-1βKO mice developed liver tumors. (G) Staining of liver sections from PGC-1$\beta^{fl/fl}$ and LivPGC-1βKO mice with H&E and PCNA (magnification, 200×). (H) Bar graphs indicate percentage of PCNA-positive area per field. (I) Relative CyclinE expression evaluated by real-time qPCR in liver specimens of PGC-1$\beta^{fl/fl}$ and LivPGC-1βKO mice treated with DEN, using Tbp as a housekeeping gene. Comparison of WT and transgenic mice (n = 12) was performed using a Student *t* test followed by Mann-Witney U test. Results are expressed as mean ± SEM (*$P < 0.05$; **$P < 0.01$). Abbreviation: CcnE1, cyclin E1.

nuclei in LivPGC-1βKO mice tumors, thus indicating large extent of genomic DNA damage. Overall, these results pinpoint to a novel scenario in which PGC-1β may play a role in promoting inflammation and, subsequently, liver carcinogenesis.

Discussion

The PGC-1s coactivators are considered master regulators of mitochondrial biogenesis and oxidative metabolism as well as of antioxidant defense. Although, in many tissues, the functions of the two major members of the family, PGC-1α and PGC-1β, are mainly redundant, in the liver they exert opposite roles. PGC-1α is involved in gluconeogenesis and lipid oxidation, whereas PGC-1β rather promotes *de novo* lipogenesis and TG secretion. Given the crucial function of the PGC-1s coactivators in the regulation of cellular metabolism, and as altered metabolism is presently considered a hallmark of cancer, the aim of our study was to examine the role of PGC-1β in a murine model of HCC. Herein, we provide evidence on the involvement of PGC-1β in hepatocarcinogenesis, by promoting antioxidant response, and therefore limiting detrimental ROS accumulation. It is therefore

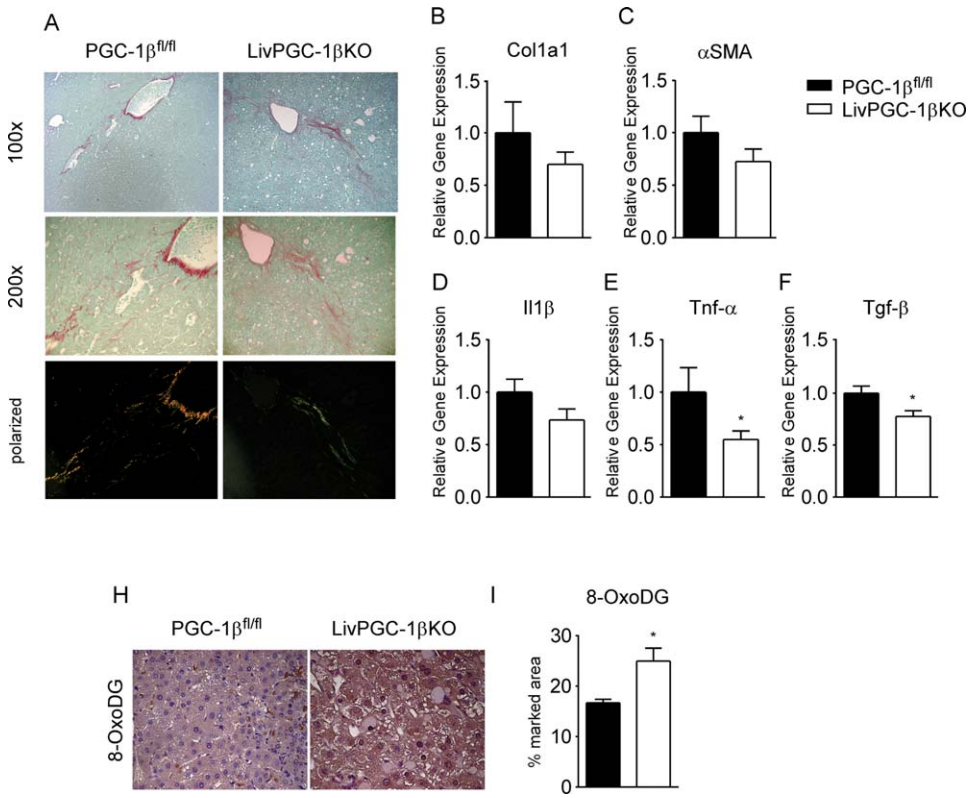

FIG. 7. Lack of hepatic PGC-1β results in less collagen deposition and impaired antioxidant response in tumors. (A) Sirius Red staining and (B) Col1a1 expression in LivPGC-1βKO mice than PGC-1$\beta^{fl/fl}$ controls group. LivPGC-1βKO tumors displayed decreased HSC activation, as indicated by (C) αSma expression. Inflammatory response, indicated by (D) Il1β, (E) Tnf-α, and (F) Tgf-β, is impaired in LivPGC-1βKO. (G) 8-oxo-dG levels were evaluated by immunohistochemistry (magnification, 400×). (H) Bar graphs indicate percentage of 8-Oxo-dG-positive area per field. Relative gene expression was evaluated in liver specimens from WT mice and LivPGC-1β mice by real-time qPCR, using Tbp as a housekeeping gene. Comparison of PGC-1$\beta^{fl/fl}$ and LivPGC-1βKO mice (n = 12) was performed using a Student *t* test followed by Mann-Witney U test. Results are expressed as mean ± SEM (*$P < 0.05$).

important to note that PGC-1β actively supports tumor cells survival not only by reprogramming metabolism to meet the bioenergetics and biosynthetic demands of rapid cell growth, but also by providing protection against stresses induced by an unfavorable microenvironment.

The key role of PGC-1β in promoting lipogenesis[11,13] is confirmed in our tumor model. Surprisingly, hepatic-specific PGC-1β ablation does not impair fatty acid synthesis, suggesting the existence of coping mechanisms able to sustain new lipid production. Furthermore, it is plausible to assume that tumor cells lacking PGC-1β could promote lipogenesis in order to counteract ROS-driven lipid peroxidation. In fact, we have shown that the hepatic-specific ablation of PGC-1β lowers the antioxidant response, resulting in the accumulation of ROS damaged DNA. Thus, we can bona fide assume the occurrence of a compensatory increase in lipid anabolism under oxidative stress conditions. After all, it has been already demonstrated that *de novo* fatty acid synthesis rescues cancer cells from oxidative stress–induced cell death.[29] It is worth recalling that the final effect of the balance between lipogenesis and antioxidant defense would reflect the status of the intracellular nicotinamide adenine dinucleotide phosphate (NADPH) pool.[30] Upon ablation of PGC-1β, the decrease in the ROS scavenging apparatus, while sparing NADPH for lipogenesis, would not be sufficient to protect cancer cells from oxidative damage and cell death.[31]

Overall, by using gain- and loss-of-function approaches, we identified the coactivator PGC-1β, as

a crucial regulator of metabolism reprogramming in cancer cells. This is achieved by fulfilling biosynthetic and bioenergetic cellular needs through the up-regulation of lipid synthesis, tricarboxylic acid cycle, and oxidative phosphorylation. Furthermore, it is not unexpected that PGC-1β exerts a tight control of ROS homeostasis, on one hand, to counterbalance ROS specimens produced by the increase in mitochondrial respiratory activity, thus promoting cell survival, and, on the other hand, to maintain a limited ROS flux to allow additional mutations and adaptations to further trigger cancer progression.[19,32,33] On the same line, it has been proposed that upon metabolic inhibition, or through the blocking of certain antioxidant systems, cancer cells are more sensitized toward programmed cell death.[34-37] In this study, we propose a scenario in which fine-tuning of mitochondrial function, redox status, and lipid metabolism modulates the postinitiation phase of liver injury and hepatocarcinogenesis, thus opening bona-fide avenues in the pathogenesis and pharmacopeia of HCC.

Acknowledgment: We thank Dr. A.K. Groen for providing the *Abcb4*$^{-/-}$ mice.

REFERENCES

1) El-Serag HB. Hepatocellular carcinoma. N Engl J Med 2011; 365:1118-1127.
2) Pavlova NN, Thompson CB. The emerging hallmarks of cancer metabolism. Cell Metab 2016;23:27-47.
3) Cairns RA, Harris IS, Mak TW. Regulation of cancer cell metabolism. Nat Rev Cancer 2011;11:85-95.
4) Hanahan D, Weinberg RA. Hallmarks of cancer: the next generation. Cell 2011;144:646-674.
5) Lin J, Handschin C, Spiegelman BM. Metabolic control through the PGC-1 family of transcription coactivators. Cell Metab 2005;1:361-370.
6) Lehman JJ, Barger PM, Kovacs A, Saffitz JE, Medeiros DM, Kelly DP. Peroxisome proliferator-activated receptor gamma coactivator-1 promotes cardiac mitochondrial biogenesis. J Clin Invest 2000;106:847-856.
7) Wu Z, Puigserver P, Andersson U, Zhang C, Adelmant G, Mootha V, et al. Mechanisms controlling mitochondrial biogenesis and respiration through the thermogenic coactivator PGC-1. Cell 1999;98:115-124.
8) Puigserver P, Wu Z, Park CW, Graves R, Wright M, Spiegelman BM. A cold-inducible coactivator of nuclear receptors linked to adaptive thermogenesis. Cell 1998;92:829-839.
9) Lin J, Wu H, Tarr PT, Zhang CY, Wu Z, Boss O, et al. Transcriptional co-activator PGC-1 alpha drives the formation of slow-twitch muscle fibres. Nature 2002;418:797-801.
10) Puigserver P, Rhee J, Donovan J, Walkey CJ, Yoon JC, Oriente F, et al. Insulin-regulated hepatic gluconeogenesis through FOXO1-PGC-1alpha interaction. Nature 2003;423:550-555.
11) Bellafante E, Murzilli S, Salvatore L, Latorre D, Villani G, Moschetta A. Hepatic-specific activation of peroxisome proliferator-activated receptor gamma coactivator-1beta protects against steatohepatitis. Hepatology 2013;57:1343-1356.
12) Maeda S, Kamata H, Luo JL, Leffert H, Karin M. IKKbeta couples hepatocyte death to cytokine-driven compensatory proliferation that promotes chemical hepatocarcinogenesis. Cell 2005;121:977-990.
13) Lin J, Yang R, Tarr PT, Wu PH, Handschin C, Li S, et al. Hyperlipidemic effects of dietary saturated fats mediated through PGC-1beta coactivation of SREBP. Cell 2005;120:261-273.
14) **Paszek MJ**, **Zahir N**, Johnson KR, Lakins JN, Rozenberg GI, Gefen A, et al. Tensional homeostasis and the malignant phenotype. Cancer Cell 2005;8:241-254.
15) Bataller R, Brenner DA. Liver fibrosis. J Clin Invest 2005;115: 209-218.
16) Pellicoro A, Ramachandran P, Iredale JP, Fallowfield JA. Liver fibrosis and repair: immune regulation of wound healing in a solid organ. Nat Rev Immunol 2014;14:181-194.
17) Wiseman H, Halliwell B. Damage to DNA by reactive oxygen and nitrogen species: role in inflammatory disease and progression to cancer. Biochem J 1996;313(Pt 1):17-29.
18) Liou GY, Storz P. Reactive oxygen species in cancer. Free Radic Res 2010;44:479-496.
19) DeNicola GM, Karreth FA, Humpton TJ, Gopinathan A, Wei C, Frese K, et al. Oncogene-induced Nrf2 transcription promotes ROS detoxification and tumorigenesis. Nature 2011;475:106-109.
20) Bellafante E, Morgano A, Salvatore L, Murzilli S, Di TG, D'Orazio A, et al. PGC-1beta promotes enterocyte lifespan and tumorigenesis in the intestine. Proc Natl Acad Sci U S A 2014; 111:E4523-E4531.
21) Beloribi-Djefaflia S, Vasseur S, Guillaumond F. Lipid metabolic reprogramming in cancer cells. Oncogenesis 2016;5:e189.
22) Kawashima M, Iwamoto N, Kawaguchi-Sakita N, Sugimoto M, Ueno T, Mikami Y, et al. High-resolution imaging mass spectrometry reveals detailed spatial distribution of phosphatidylinositols in human breast cancer. Cancer Sci 2013;104:1372-1379.
23) **Ide Y**, **Waki M**, Hayasaka T, Nishio T, Morita Y, Tanaka H, et al. Human breast cancer tissues contain abundant phosphatidylcholine(36ratio1) with high stearoyl-CoA desaturase-1 expression. PLoS One 2013;8:e61204.
24) Bakiri L, Wagner EF. Mouse models for liver cancer. Mol Oncol 2013;7:206-223.
25) Davit-Spraul A, Gonzales E, Baussan C, Jacquemin E. The spectrum of liver diseases related to ABCB4 gene mutations: pathophysiology and clinical aspects. Semin Liver Dis 2010;30:134-146.
26) Katzenellenbogen M, Mizrahi L, Pappo O, Klopstock N, Olam D, Jacob-Hirsch J, et al. Molecular mechanisms of liver carcinogenesis in the mdr2-knockout mice. Mol Cancer Res 2007;5:1159-1170.
27) Moustafa T, Fickert P, Magnes C, Guelly C, Thueringer A, Frank S, et al. Alterations in lipid metabolism mediate inflammation, fibrosis, and proliferation in a mouse model of chronic cholestatic liver injury. Gastroenterology 2012;142:140-151.
28) Katzenellenbogen M, Pappo O, Barash H, Klopstock N, Mizrahi L, Olam D, et al. Multiple adaptive mechanisms to chronic liver disease revealed at early stages of liver carcinogenesis in the Mdr2-knockout mice. Cancer Res 2006;66:4001-4010.
29) Rysman E, Brusselmans K, Scheys K, Timmermans L, Derua R, Munck S, et al. De novo lipogenesis protects cancer cells from free radicals and chemotherapeutics by promoting membrane lipid saturation. Cancer Res 2010;70:8117-8126.
30) Jeon SM, Chandel NS, Hay N. AMPK regulates NADPH homeostasis to promote tumour cell survival during energy stress. Nature 2012;485:661-665.

31) Nelson ME, Lahiri S, Chow JD, Byrne FL, Hargett SR, Breen DS, et al. Inhibition of hepatic lipogenesis enhances liver tumorigenesis by increasing antioxidant defence and promoting cell survival. Nat Commun 2017;8:14689.
32) Jin L, Li D, Alesi GN, Fan J, Kang HB, Lu Z, et al. Glutamate dehydrogenase 1 signals through antioxidant glutathione peroxidase 1 to regulate redox homeostasis and tumor growth. Cancer Cell 2015;27:257-270.
33) Piskounova E, Agathocleous M, Murphy MM, Hu Z, Huddlestun SE, Zhao Z, et al. Oxidative stress inhibits distant metastasis by human melanoma cells. Nature 2015;527):186-191.
34) Raj L, Ide T, Gurkar AU, Foley M, Schenone M, Li X, et al. Selective killing of cancer cells by a small molecule targeting the stress response to ROS. Nature 2011;475:231-234.
35) Bhardwaj R, Sharma PK, Jadon SP, Varshney R. A combination of 2-deoxy-D-glucose and 6-aminonicotinamide induces cell cycle arrest and apoptosis selectively in irradiated human malignant cells. Tumour Biol 2012;33:1021-1030.
36) Hanot M, Boivin A, Malesys C, Beuve M, Colliaux A, Foray N, et al. Glutathione depletion and carbon ion radiation potentiate clustered DNA lesions, cell death and prevent chromosomal changes in cancer cells progeny. PLoS One 2012;7:e44367.
37) Sturlan S, Baumgartner M, Roth E, Bachleitner-Hofmann T. Docosahexaenoic acid enhances arsenic trioxide-mediated apoptosis in arsenic trioxide-resistant HL-60 cells. Blood 2003;101:4990-4997.
38) Lelliott CJ, Medina-Gomez G, Petrovic N, Kis A, Feldmann HM, Bjursell M, et al. Ablation of PGC-1beta results in defective mitochondrial activity, thermogenesis, hepatic function, and cardiac performance. PLoS Biol 2006;4:e369.

Author names in bold designate shared co-first authorship.

Supporting Information

Additional Supporting Information may be found at onlinelibrary.wiley.com/doi/10.1002/hep.29484/suppinfo